Supporting information

“High resolution patterning of PbS quantum dots/graphene photodetectors with high responsivity via photolithography with top graphene layer to protect surface ligands”

Seungbae Ahn, Wenjun Chen, and Oscar Vazquez-Mena*

Department of Nanoengineering, Center for Memory and Recording Research, Calibaja Center for Resilient Materials and Systems, University of California San Diego, 9500 Gilman Drive, La Jolla, CA, 92093, USA

E-mail: oscarvm@eng.ucsd.edu

Dr. Oscar Vazquez Mena

NanoEngineering Department, University of California San Diego,

9500 Gilman Drive, La Jolla, CA, 92093, USA

Keywords: Quantum dot patterning, graphene passivation, photolithography, optoelectronics

Supporting information content

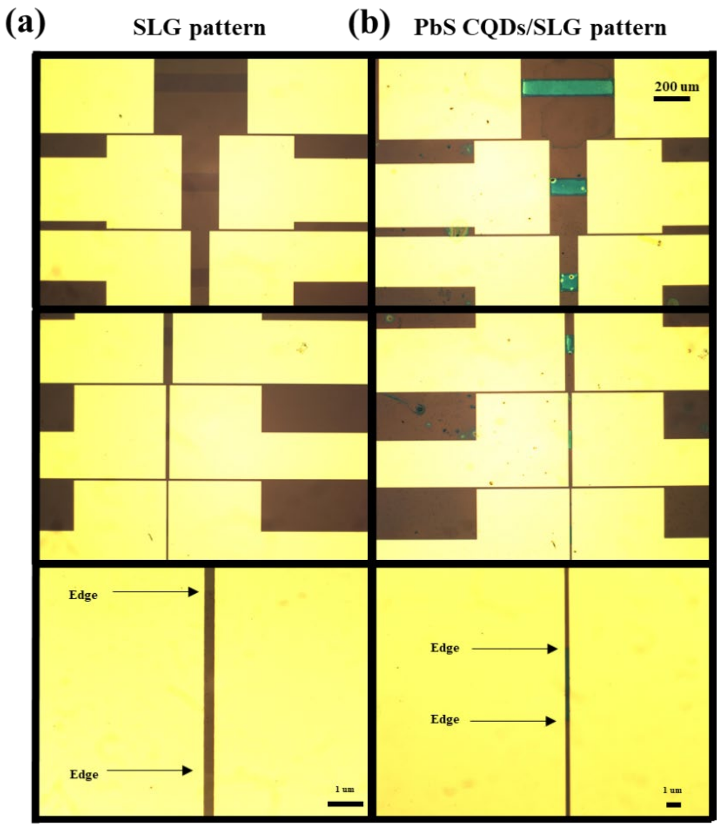

Figure SI.1. a) Optical images of pattered SLG. The length of SLG is 500, 200, and 100 μm in first row from top to bottom, respectively, and 50, 20, and 10 μm in second row, from top to bottom, respectively, and 5 μm in third row and the width of all SLG channel is 100 μm. b) Optical images of patterned PbS CQDs on patterned SLG.

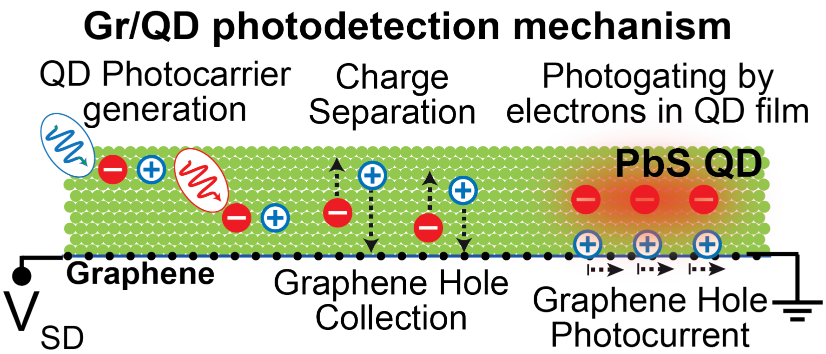

Figure SI.2. Light is absorbed by QDs generating photocarriers, followed by charge separation. In the specific case of Gr and PbS-QDs, due to band alignment and interface built-in potential, electrons stay in the QDs while holes are transferred to graphene. The transferred holes change the graphene (p-type) conductivity while the electrons generate a photogating effect.

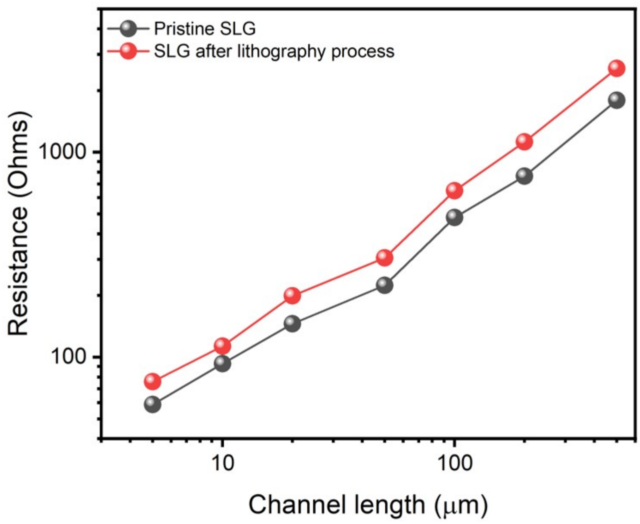

Figure SI. 3. The resistance of various lengths SLG before and after lithography process.

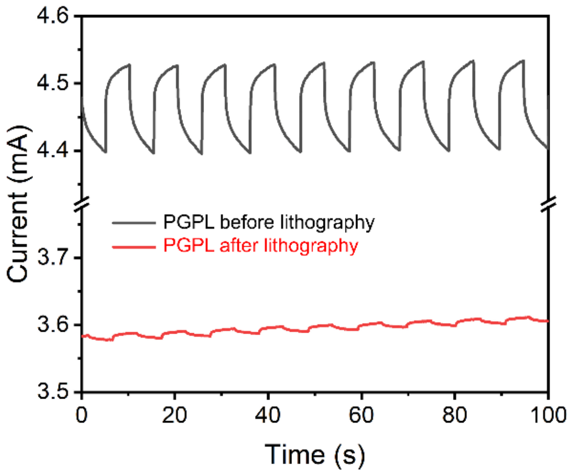

Figure SI.4 Photoresponse: PGPL before and after lithography. These results clearly show the use of lithography without the PGPL result in significant degradation of the photoresponse. Adding the PGPL with the top graphene layer after the lithography does not show any significant enhancement since the QD ligands are already damaged.

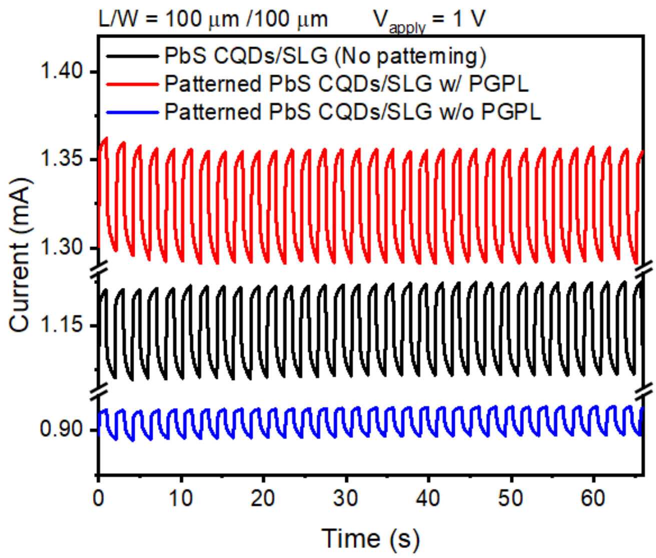

Figure SI.5. The 60-seconds time traces show the stability of the photoresponse.

<table>
<tr><td colspan="2">Figure SI.6. Calculation of detectivity at incident light power of 1.6x10-8 mW at 40, 10 and 2 Hz.</td></tr>
<tr><td colspan="2">Device dimensions: Device Area (A_d): $(100\mu m)^2$=0.0001 cm^2</td></tr>
<tr><td>Dark current trace at Δf=40 Hz:
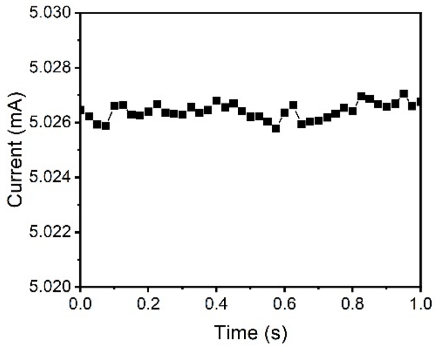
</td><td>Responsivity at 40 Hz: 7.32x10^6 A/W

Current RMS noise at 40 Hz: 292 nA

NEP=$Noise_{rms}$/Responsivity=3.99x10^{-14} W

Detectivity: $D^* = \frac{\sqrt{\Delta f\, A_d}}{NEP}$ = 1.59x10^{12} Jones</td></tr>
<tr><td>Dark current trace at Δf=10 Hz:
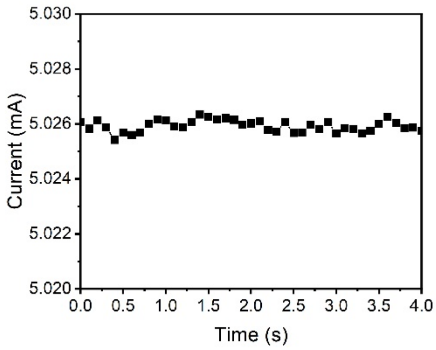
</td><td>Responsivity at 10 Hz: 9.34x10^6 A/W

Current RMS noise at 20 Hz: 210 nA

NEP=$Noise_{rms}$/Responsivity=2.25x10^{-14} W

Detectivity: $D^* = \frac{\sqrt{\Delta f\, A_d}}{NEP}$ = 1.41x10^{12} Jones</td></tr>
<tr><td>Dark current trace at Δf=2 Hz
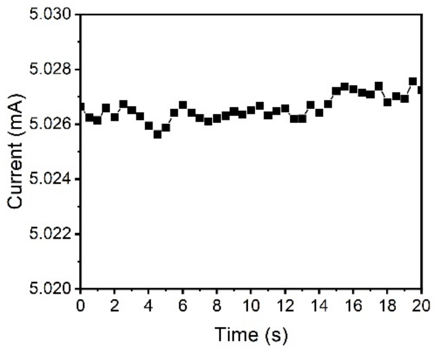
</td><td>Responsivity at 2 Hz: 1.28x10^7 A/W

Current RMS noise at 20 Hz: 441 nA

NEP=$Noise_{rms}$/Responsivity=3.45x10^{-14} W

Detectivity: $D^* = \frac{\sqrt{\Delta f\, A_d}}{NEP}$ = 0.41x10^{12} Jones</td></tr>
</table>

UV/Vis before and after ligand exchange.

Photocurrent before and after ligand exchange

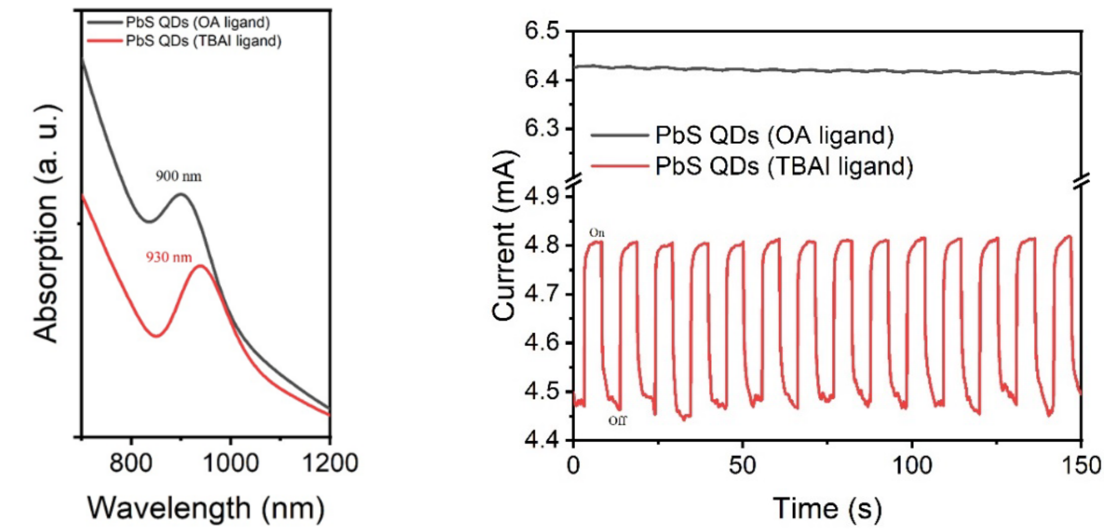

Figure SI.7 UV/Vis absorption and photocurrent before and after ligand exchange from oleic acid (OA) to TBAI. Ligand exchange is crucial to facilitate the charge transport along the QD film and therefore the charge collection by the SLG. The ligand exchange induces a red-shift in the absorption. However, the photocurrent is drastically improved after the ligand exchange, showing the importance of the surface ligands ligand exchange.